Journal of the Ceramic Society of Japan 123 [7] 570-575 2015 Paper

Pressureless sintering of SiC-coated carbon nanofiber/SiC composites and their properties

Guosheng XU,[*,] Tomohiko YAMAKAMI,[*] Tomohiro YAMAGUCHI,[*] Morinobu ENDO,[*] Seiichi TARUTA[*,†] and Isao KUBO[**]**

[*]**Faculty of Engineering, Shinshu University, 4–17–1 Wakasato, Nagano 380–8553, Japan**
[**]**Fine ceramics division, ASUZAC Inc., 981 Nakayama, Takayama-mura, Kamitakai-gun, Nagano 382–8508, Japan**

In this study, in order to improve interfacial strength between CNFs and SiC matrix and to disperse CNFs uniformly in the SiC matrix, using the SiC-coated CNFs which were prepared using SiO_2 powder at 1400–1800°C in argon atmosphere, CNFs/SiC composites were fabricated in argon atmosphere under pressureless condition. The non-coated CNFs/SiC and SiC-coated CNFs/SiC composites reached near the full density at 2150°C. The SiC grains and the carbon agglomerates in the composites tended to be finer with an increase in amount of SiC coating on CNFs. The SiC-coated CNFs/SiC composites showed almost the same fracture toughness (4.5–5.0 MPa·m$^{0.5}$) with the non-coated CNFs/SiC composite. On the other hand, the SiC-coated CNFs/SiC composites showed higher bending strength than the non-coated CNFs/SiC composite, and the bending strength became higher with an increase in amount of SiC coating on CNFs. The maximum bending strength was 551 MPa, which represent a 32% increase compared with that of the non-coated CNFs/SiC composite.

©2015 The Ceramic Society of Japan. All rights reserved.

Key-words : Carbon nanofibers, SiC coating, SiC, Composite, Mechanical properties, Densification, Microstructure

[Received February 21, 2015; Accepted April 19, 2015]

1. Introduction

Pressureless sintering for SiC ceramics was first performed using a small amounts of B and C as sintering aids by Prochazka.[1] It is now one of the industrial manufacturing method of SiC ceramics. Such SiC ceramics are densified through a solid-phase sintering, and their fracture toughness is usually 2–3 MPa·m$^{0.5}$,[2),3)] which is lower than the fracture toughness of SiC ceramics densified through a liquid-phase sintering using a large amount of sintering aids. However, such liquid-phase sintered SiC ceramics cannot be applied to the chambers and trays of the semiconductor fabricating equipment because the SiC ceramics applied to such chambers and trays are required ppm order in the content of the impurities, particularly metal elements.

In our previous study,[4)] 3 wt% carbon nanofibers (CNFs)/SiC composite, which was fabricated by pressureless sintering using a small amounts of B_4C as sintering aids, showed 50% increase in the fracture toughness, compared with the solid-phase sintered monolithic SiC. The improved fracture toughness resulted from the pullout and/or bridging effects of CNFs bonded with SiC grains much more tightly. On the other hand, the bending strength of the 3 wt%-CNFs/SiC composite was just a little higher than that of the monolithic SiC because the addition of 3 wt% CNTs might make the fracture origin larger.

If CNFs can be coated uniformly with SiC layer, the layer may strengthen the interface bonding between CNFs and SiC matrix and enhance the dispersibility of CNFs, which will improve not only fracture toughness but also bending strength. In our previous study,[5)] the SiC coating on CNFs was performed at 1400–1800°C in argon atmosphere using SiO_2, SiO and mixture of Si and SiO_2 powders (Si/SiO_2 powder) as silicon sources, and the modification and dispersibility of the treated CNFs were investigated. So we found that β-SiC particles were deposited on the CNFs in all the specimens at 1600–1800°C, and the dispersibilities of the SiC-coated CNFs were superior to those of as-received CNFs and oxidized CNFs.

Morisada et al. reported that the SiC coating was formed on CNTs by heating CNTs with SiO powder in vacuum.[6)–8)] The SiC-coated CNFs was actually combined with SiC by pulsed electric current sintering and they increased the fracture toughness of the obtained composites.[9)] However, Morisada et al. did not reported on the densification behavior and microstructure development of the obtained composites in detail.

In this study, in order to improve interfacial strength between CNFs and SiC matrix and to disperse CNFs uniformly in the SiC matrix, using the SiC-coated CNFs which were prepared using SiO_2 powder at 1400–1800°C in argon atmosphere, CNFs/SiC composites were fabricated in argon atmosphere under pressureless condition. The densification behavior, microstructure development and mechanical properties of the obtained SiC-coated CNFs/SiC composites were compared with those of non-coated CNFs/SiC composite.

2. Experimental procedure

2.1 SiC-coated CNFs

CNFs used in this study were vapor-grown carbon fibers (VGCF, Showa Denko, Japan), which are a type of multi walled carbon nanotubes. The diameter and length were 150 nm and 8 μm, respectively.

SiC coating on the CNFs was performed at 1400–1800°C in argon atmosphere using SiO_2, SiO and Si/SiO_2 powders as silicon sources, in the previous study.[5)] β-SiC particles were deposited on the CNFs in all the specimens prepared at 1600–1800°C. Their XRD patterns are shown in the previous paper.[5)] SiC deposited on the CNFs using SiO_2 were less than that deposited on the CNFs using other silicon sources, particularly the SiC deposited on the

† Corresponding author: S. Taruta; E-mail: staruta@shinshu-u.ac.jp

©2015 The Ceramic Society of Japan
DOI http://dx.doi.org/10.2109/jcersj2.123.570

CNFs using SiO_2 at 1400°C were very little. Nevertheless, the SiC-coated CNFs prepared using SiO_2 at 1400, 1600 and 1800°C were used in this study because the CNFs had a fewer defects. The CNFs coated with more SiC had more defects,[5] and so the strength of such CNFs should be weaker.[10]

The SiC-coated CNFs prepared using SiO_2 at 1400, 1600 and 1800°C are shown as 1400-coated CNFs, 1600-coated CNFs and 1800-coated CNFs, respectively, in this paper. The SiC deposited on the CNFs increased with an increase in the preparing temperature of the coating, as mentioned in the previous paper.[5] As non-coated CNFs, the CNFs oxidized in $NaClO_3$ solution[4),5] were used in this study. The surface of the oxidized CNFs became hydrophilic, and so they had better dispersibility than the pristine CNFs.[5]

2.2 Fabrication of SiC-coated CNFs/SiC composites

The SiC-coated CNFs were added to the distilled water in which ammonium naphthalene sulfonate was dissolved as a dispersant, and dispersed by ultrasonic for 1 h. The mixtures were treated by ball milling for 24 h after their pH was adjusted to 11 using tetra-methyl ammonium hydroxide. The obtained SiC-coated CNFs suspension was mixed with α-SiC powder (OY-15, average particle size 0.7 μm, purity 98.7%, Yakushima Denko) and B_4C (Wacker-Chemie GmbH, Germany) which was sintering aid of SiC by ball milling for 24 h. The SiC-coated CNFs content in the obtained powder mixtures was 3 wt % and the B_4C content was 0.7 wt %. In order to make the mixtures gels, the epoxy resin (1,2,3-propanetriol glycidyl ether) and the initiator [polypropylene glycol bis (aminopropyl) ether] were added to the obtained slurries. The slurries were degassed, casted in mold and then heated at 40°C for 3 h. The obtained gels with the size of 100 mm × 100 mm × 10 mm were dried at 90°C and calcined at 600°C for 2 h in vacuum to thermally decompose the epoxy resin and the initiator. The calcined gels were sintered at 2050–2150°C for 2 h in argon atmosphere under pressureless condition. In this way, 1400-coated CNFs/SiC, 1600-coated CNFs/SiC and 1800-coated CNFs/SiC composites were fabricated. The non-coated CNFs/SiC composite was also fabricated in the same way.

2.3 Estimation of SiC-coated CNFs/SiC composites

The bulk densities of the composites were measured by Archimedes method. The relative densities were calculated using the bulk densities of the composites and the theoretical densities of SiC (3.21 g/cm^3) and VGCF (2.1 g/cm^3). Their microstructures were observed using a scanning electron microscopy (SEM) and a transmission electron microscopy (TEM). The SEM images of polished surfaces were observed using electron beam under low accelerating voltage of 3 kV, and those of fracture surfaces were observed using electron beam under accelerating voltage of 15 kV.

The mechanical properties, bending strength, fracture toughness, Vickers hardness and Young's modulus of the obtained composites, were measured by the same methods with those used in the previous study.[4] The bending strength of the composites with size of 4 mm × 3 mm × 40 mm was measured by a three-point bending test, with a crosshead speed of 0.5 mm/min and a span length of 30 mm. The fracture toughness of the composites was measured by indentation fracture (IF) method.

The SiC grain sizes of the composites which were polished and thermally etched at 350°C lower temperatures than the sintering temperatures for 2 h were measured on the SEM photographs by the line-intercept method. The average SiC grain size was determined from the sizes of about 200 grains.

3. Results and discussion

3.1 Densification and microstructure development

SiC crystal phases in the obtained CNFs/SiC composites were α-type consisting of 6H, 15R, 4H, 33R and 21R phase. Though SiC crystal phase deposited on the CNFs was β-type, it was not detected when the composites were analyzed using X-ray diffractometric analyzer.

The relative densities of the non-coated CNFs/SiC, 1400-coated CNFs/SiC, 1600-coated CNFs/SiC and 1800-coated CNFs/SiC composites sintered at 2050–2150°C are shown in **Fig. 1**. All the composites were not sufficiently densified below 2100°C, and reached near the full density at 2150°C. The relative densities of the composites tended to be higher with an increase in amount of SiC coating on CNFs, particularly, the 1800-coated CNFs/SiC composite had much higher relative density at 2050 and 2100°C than other composites.

SEM images of the polished surfaces of the non-coated CNFs/SiC, 1400-coated CNFs/SiC, 1600-coated CNFs/SiC and 1800-coated CNFs/SiC composites sintered at 2150°C are shown in **Fig. 2**. As these SEM images were observed using electron beam under low accelerating voltage of 3 kV, the size and shape of SiC grains could be confirmed in the SEM images. SiC grains in such composites are equi-axial shape. However, the SiC grains in the SiC-coated CNFs/SiC composites, particularly in the 1800-coated CNFs/SiC composite, seemed to be smaller than those in the non-coated CNFs/SiC composite. The average SiC grain sizes of the composites sintered at 2150°C are shown in **Fig. 3**. The average SiC grain size of the non-coated CNFs/SiC composite was around 6 μm, which was a little smaller than that of the 1400-coated CNFs/SiC composite. And the average SiC grain size of the SiC-coated CNFs/SiC composites decreased with an increase in amount of SiC coating on CNFs, and that of the 1800-coated CNFs/SiC composite were much smaller than that of the non-coated CNFs/SiC composite.

Most of dark parts observed in Fig. 2 contained carbon agglomerates consisting of residual carbons and CNFs, as shown in the previous study.[4] The residual carbons were formed by thermal decomposition of epoxy resin and initiator during

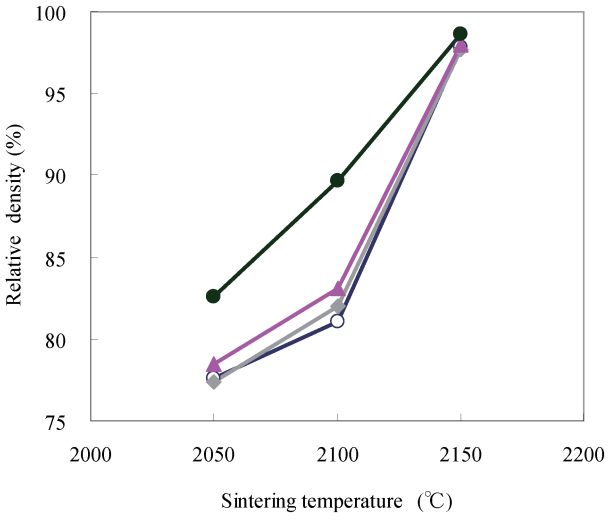

Fig. 1. Relative densities of (○) non-coated CNFs/SiC, (◆) 1400-coated CNFs/SiC, (▲) 1600-coated CNFs/SiC and (●) 1800-coated CNFs/SiC composites sintered at 2050–2150°C.

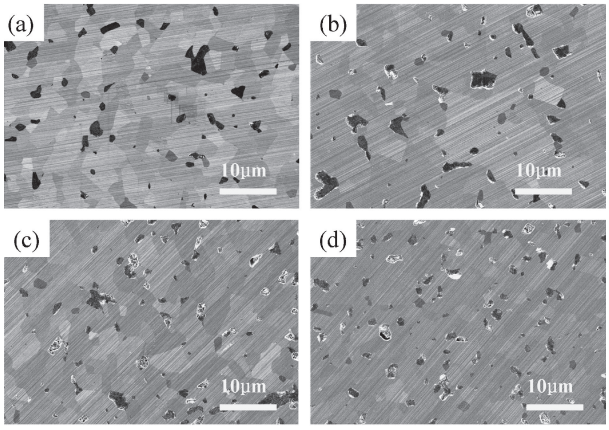

Fig. 2. SEM images of polished surfaces of (a) non-coated CNFs/SiC, (b) 1400-coated CNFs/SiC, (c) 1600-coated CNFs/SiC and (d) 1800-coated CNFs/SiC composites sintered at 2150°C.

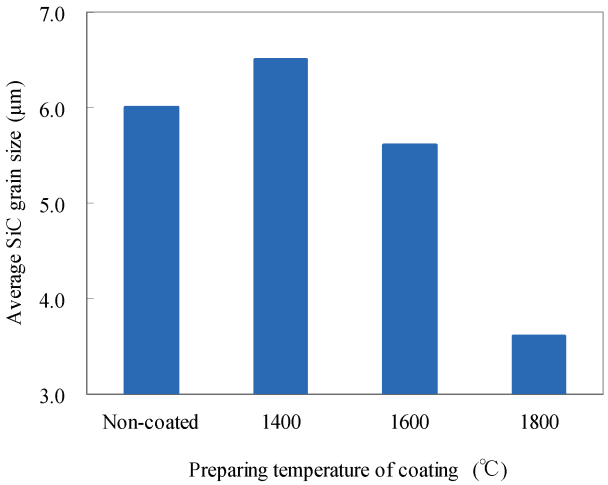

Fig. 3. Average SiC grain sizes of non-coated CNFs/SiC, 1400-coated CNFs/SiC, 1600-coated CNFs/SiC and 1800-coated CNFs/SiC composites sintered at 2150°C.

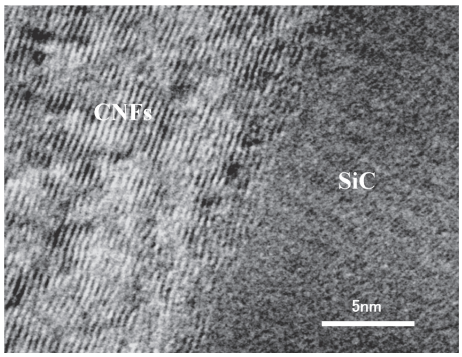

Fig. 4. TEM image of interface between CNFs and SiC grain in 1600-coated CNFs/SiC composite sintered at 2150°C.

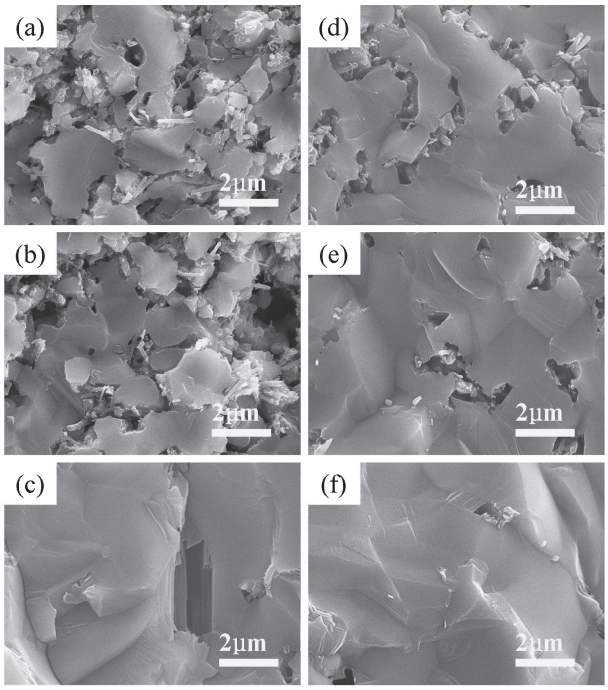

Fig. 5. SEM images of fracture surfaces of non-coated CNFs/SiC composites sintered at (a) 2050°C, (b) 2100°C and (c) 2150°C and 1800-coated CNFs/SiC composites sintered at (d) 2050°C, (e) 2100°C and (f) 2150°C.

calcination in vacuum. The sizes of these dark parts, namely carbon agglomerates, in the non-coated CNFs/SiC, 1400-coated CNFs/SiC and 1600-coated CNFs/SiC composites were less than 5 μm, and the sizes of the carbon agglomerates in the 1800-coated CNFs/SiC composite were about 2 μm. In this way, the growth of the carbon agglomerates were inhibited as well as the growth of SiC grains by using CNFs coated with more SiC.

TEM image of the interface between CNF and SiC grain in the 1600-coated CNFs/SiC composite sintered at 2150°C is shown in **Fig. 4**. The inner-walls of CNFs were observed clearly, and apertures and second phases were not observed at the interface. In addition, the interface was unclear. So this TEM image indicates that the CNFs and the SiC grains were bonded much more tightly.

SEM images of the fracture surfaces of the non-coated CNFs/SiC and 1800-coated CNFs/SiC composites sintered at 2050–2150°C are shown in **Fig. 5**. Below 2100°C, the SiC matrix in the 1800-coated CNFs/SiC composites [Figs. 5(d) and 5(e)] were densified partially much more, compared with that of the non-coated CNFs/SiC composite [Figs. 5(a) and 5(b)]. At 2150°C, both the non-coated CNFs/SiC composite and the 1800-coated CNFs/SiC composite were densified fully. Though SiC grains in the 1800-coated CNFs/SiC composite sintered at 2150°C were smaller than those in the non-coated CNFs/SiC composite sintered at 2150°C, those in the 1800-coated CNFs/SiC composite sintered at 2050–2100°C were larger than those in the non-coated CNFs/SiC composite sintered at the same temperature. Such difference in the sintering behavior between the non-coated CNFs/SiC composites and the 1800-coated CNFs/SiC composites might result from the difference in the dispersibility between the 1800-coated CNFs and the non-coated CNFs. The dispersibility of CNFs became higher in the water of pH = 10 with an increase in amount of SiC coating on CNFs.[5] So the dispersibility of the SiC-coated CNFs, particularly the 1800-coated CNFs, were superior to that of the non-coated CNFs. Therefore, the 1800-coated CNFs could be dispersed more uniformly in SiC matrix and so the SiC matrix was densified more uniformly and the grain growth of SiC also progressed more uniformly at lower temperatures of 2050–2100°C, as shown in Figs. 5(d) and 5(e). On the other side, the non-coated CNFs might not be dispersed more uniformly. Therefore, only inside of SiC agglomerates in which just a few CNFs were distributed was first densified at lower temperatures

Table 1. Mechanical properties and calculated sizes (2c) of fracture origins for monolithic SiC, non-coated CNFs/SiC composite and SiC-coated CNFs/SiC composites sintered at 2150°C

Specimen	CNFs content (wt %)	Relative density (%)	Vickers hardness (GPa)	Young modulus (GPa)	Fracture toughness ($MPa \cdot m^{0.5}$)	Bending strength (MPa)	Size of fracture origin (μm)
Monolithic SiC ceramic	0	98.8	22.7	425.8	3.3 ± 0.2	397 ± 15	44
Non-coated CNFs/SiC composite	3	98.1	25.0	387.0	5.0 ± 1.3	420 ± 42	90.4
1400-coated CNFs/SiC composite	3	97.7	19.8	387.9	4.5 ± 0.5	426 ± 19	71.1
1600-coated CNFs/SiC composite	3	98.0	19.2	385.2	5.0 ± 0.2	476 ± 36	70.3
1800-coated CNFs/SiC composite	3	98.6	21.3	398.1	4.5 ± 0.3	554 ± 41	42.0

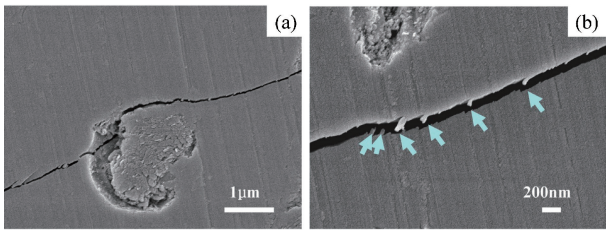

Fig. 6. SEM images of Vickers crack on the surface of 1800-coated CNFs/SiC composite sintered at 2150°C. (a) low magnification and (b) high magnification.

and the grain growth of SiC progressed only inside the agglomerates, but the SiC matrix in which many CNFs were distributed was not densified and inter-dense SiC agglomerates were not also sintered. That is, non-uniform densification and non-uniform SiC grain growth occurred in the non-coated CNFs/SiC composite. Consequently, not only large SiC grains but also a lot of much smaller SiC grains were observed in Figs. 5(a) and 5(b). So when the densification of the composite progressed very rapidly at higher temperature of 2150°C, the large SiC grains, which were formed by grain growth of SiC inside the agglomerates, might grow very rapidly as the nucleus and became much larger. At the same time, the non-coated CNFs and residual carbons moved with grain boundaries, gathered at some location of SiC grain boundaries and formed larger carbon agglomerates as shown in Fig. 2(a).

3.2 Mechanical properties

The mechanical properties of the monolithic SiC, non-coated CNFs/SiC and SiC-coated CNFs/SiC composites sintered at 2150°C are shown in **Table 1**. The fracture toughnesses of the non-coated CNFs/SiC and SiC-coated CNFs/SiC composites were 4.5–5.0 $MPa \cdot m^{0.5}$. SEM images of Vickers cracks on the surface of the 1800-coated CNFs/SiC composite are shown in **Fig. 6**. The crack deflections were observed on the surface, and the bridgings and/or pull-outs of CNFs were also observed in Vickers cracks. These were also observed for the non-coated CNFs/SiC composite.[4] However, the pulled CNFs from matrix of the SiC-coated CNFs/SiC composite were cut off and were short, compared with the pulled CNFs from matrix of the non-coated CNFs/SiC composite. As mentioned at section 2.1, the defects in CNFs were increased by SiC coating, which caused the strength degradation of CNFs. Therefore, the strength of the CNFs was lowered with an increase in amount of SiC coating on CNFs. That is, though the SiC-coated CNFs might bond with the SiC matrix much more tightly, the degraded SiC-coated CNFs were easy to be cut off by crack propagation. As the results, the fracture toughness of the SiC-coated CNFs/SiC composites was almost the same with that of the non-coated CNFs/SiC composite.

Table 2. Calculated sizes (2c) of fracture origins for individual test pieces of non-coated CNFs/SiC composite measured bending strength

Test piece No.	1	2	3	4	5	Ave.
Bending strength (MPa)	440.7	364.6	409.3	454.3	430.0	419.8
Size of fracture origin (μm)	82.0	119.8	95.1	77.2	86.1	90.4

Table 3. Calculated sizes (2c) of fracture origins for individual test pieces of 1800-coated CNFs/SiC composite measured bending strength

Test piece No.	6	7	8	9	10	Ave.
Bending strength (MPa)	568.7	575.3	569.5	573.9	482.1	553.9
Size of fracture origin (μm)	39.9	39.0	39.8	39.2	55.5	42.0

On the other hand, the SiC-coated CNFs/SiC composites showed higher bending strength than the non-coated CNFs/SiC composite, and the bending strength became higher with an increase in amount of SiC coating on CNFs. That is, the bending strength tended to be higher as SiC grains in the composites were smaller. And the 1800-coated CNFs/SiC composite which had the smallest average SiC grain size showed the maximum bending strength of 551 MPa, which represented a 39% increase compared with that of the monolithic SiC and a 32% increase compared with that of the non-coated CNFs/SiC composite.

The sizes (2c) of the fracture origins for the individual test pieces measured the bending strength were calculated from the following relationship between bending strength (σ_f) and fracture toughness (K_{IC}).

$$\sigma_f = \frac{K_{IC}}{\sqrt{\pi c}} \quad (1)$$

As the fracture toughness (K_{IC}) of the non-coated CNFs/SiC and 1800-coated CNFs/SiC composites, 5.0 and 4.5 $MPa \cdot m^{0.5}$ are used, respectively and the shape factor is assumed to be 1. The results are shown in **Tables 2** and **3**. The calculated average sizes (2c) of the fracture origins for the non-coated CNFs/SiC and 1800-coated CNFs/SiC composites were 90.4 and 42.0 μm, respectively. Furthermore, the average sizes of the fracture origins for all composites were also showed in Table 1. The fracture origins in the SiC-coated CNFs/SiC composites became smaller with an increase in amount of SiC coating on CNFs. These sizes were much larger than the sizes of carbon agglomerates observed in Fig. 2. Therefore, such carbon agglomerates were not practical fracture origins. Then, the fracture surfaces of the non-coated CNFs/SiC and 1800-coated CNFs/SiC composites measured bending strength were observed using SEM.

SEM images of the fracture surfaces of test piece No.2 and No.4 having minimum bending strength (364.6 MPa) and maximum bending strength (454.3 MPa) of the non-coated CNFs/SiC composite, respectively, are shown in **Fig. 7**. The hackle, which

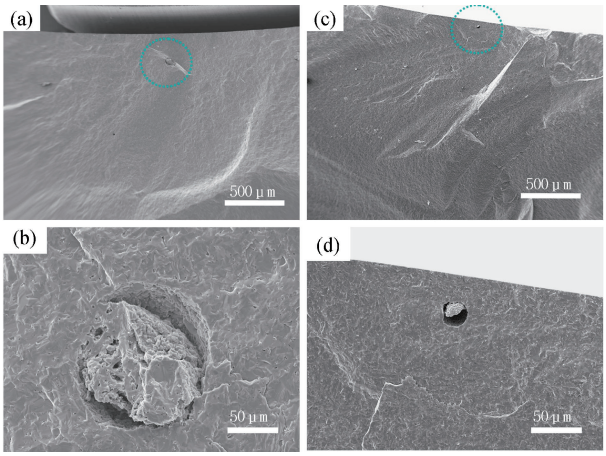

Fig. 7. SEM images of fracture surfaces of (a) and (b) test piece No.2 and (c) and (d) test piece No.4 which had minimum bending strength (364.6 MPa) and maximum bending strength (454.3 MPa) of non-coated CNFs/SiC composite, respectively.

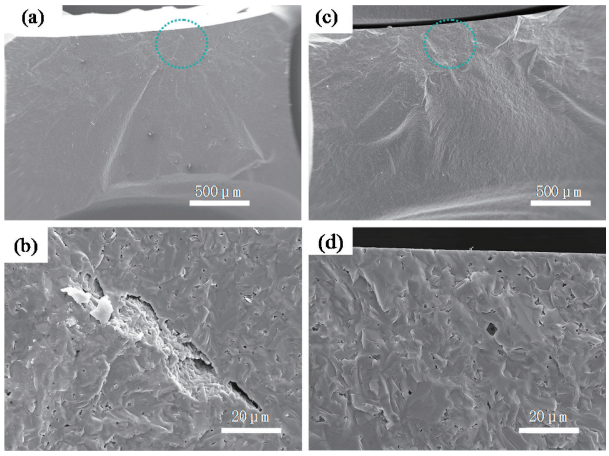

Fig. 8. SEM images of fracture surfaces of (a) and (b) test piece No.7 and (c) and (d) test piec No.10 which had maximum bending strength (575.3 MPa) and minimum bending strength (482.1 MPa) of 1800-coated CNFs/SiC composite, respectively.

was radial fracture surface, was observed on the fracture surface of test piece No.2 [Fig. 7(a)]. The large pore, which contained the aggregate particles, was observed in the center of the hackle. The size of the pore was about 100 μm, which was almost the same size with the calculated size (119.8 μm) of fracture origin. Therefore, the large pore was certainly fracture origin for test peace No.2. On the other side, the hackle was not observed clearly on the fracture surface of test piece No.4. A pore with size of about 40 μm was observed near the surface [Fig. 7(d)]. Because the pore was much smaller than calculated size of the fracture origin (77.2 μm), it could not be identified as the fracture origin for this test piece. The fracture origin for test peace No.4, which could not be found by SEM observation, might be scratches formed by grinding the surface.

SEM images of the fracture surfaces of test piece No.7 and No.10 having maximum bending strength (575.3 MPa) and minimum bending strength (482.1 MPa) of the 1800-coated CNFs/SiC composite, respectively, are shown in **Fig. 8**. The hackle was observed on the fracture surface of test piece No.10 [Fig. 8(a)]. The large crack-like pore was observed in the center of the hackle [Figs. 8(a) and 8(b)]. The size of the pore was about 60 μm in long direction, which corresponded to the calculated size (55.5 μm) of fracture origin. Therefore, the fracture origin for test peace No.10 was certainly the large crack-like pore, which might be formed by insufficient sintering, but not carbon agglomerate. On the other side, the hackle was also observed on the fracture surface of test piece No.7, however, the fracture origin such as large pore was not observed on the fracture surface. Probably, the fracture origin for test peace No.7 was scratches, which was the same with that of test peace No.4. Such large pores and scratches were a few in the composites, and they lowered the bending strength of the composites remarkably.

From the above results, it was concluded that the fracture origins for the non-coated CNFs/SiC and 1800-coated CNFs/SiC composites were large pores formed by insufficient sintering and scratches formed by grinding. The CNFs coated with more SiC were dispersed more uniformly in the composites, the microstructures of the composites became finer, and the large pores formed by insufficient sintering and the scratches formed on the surface by grinding, which acted as fracture origin, became also finer. Therefore, if such fracture origin can be much finer, the bending strength becomes much higher.

4. Conclusions

3 wt % SiC-coated CNFs/SiC composites were fabricated in argon atmosphere under pressureless condition. The densification behavior, microstructure development and mechanical properties of the obtained SiC-coated CNFs/SiC composites were compared with those of 3 wt % non-coated CNFs/SiC composite. As the results, following conclusions were obtained.

(1) The non-coated CNFs/SiC and SiC-coated CNFs/SiC composites reached near the full density at 2150°C. The SiC grains and the carbon agglomerates in the composites tended to be finer with an increase in amount of SiC coating on CNFs. The SiC grains in the composite fabricated using CNFs coated with more SiC were much smaller than those in the non-coated CNFs/SiC composite.

(2) At lower temperatures of 2050–2100°C, the densification and SiC grain growth in the composite fabricated using CNFs coated with more SiC progressed more than those in the non-coated CNFs/SiC composite. This might result from the difference in the dispersibility between the SiC-coated CNFs and the non-coated CNFs. The CNFs coated with more SiC might be dispersed more uniformly in SiC matrix and so the SiC matrix was densified more uniformly and the grain growth of SiC also progressed more uniformly.

(3) When the densification, particularly in the non-coated CNFs/SiC composite, progressed very rapidly at higher temperature of 2150°C, the large SiC grains, which were formed by grain growth of SiC in agglomerates, grew very rapidly as the nucleus and became much larger. At the same time, the CNFs and residual carbons moved rapidly with grain boundaries, gathered at some location of SiC grain boundaries and formed larger carbon agglomerates.

(4) The SiC-coated CNFs/SiC composites showed almost the same fracture toughness (4.5–5.0 $MPa \cdot m^{0.5}$) with the non-coated CNFs/SiC composite. This resulted from the increase in defect in the SiC-coated CNFs. The defect in the CNFs was increased by the SiC coating, which lowered the strength of the CNFs. That is, though the SiC-coated CNFs might bond with SiC matrix much more tightly, the degraded SiC-coated CNFs were easy to be cut off by crack propagation.

(5) The SiC-coated CNFs/SiC composites showed higher bending strength than the non-coated CNFs/SiC composite and

the bending strength became higher with an increase in amount of SiC coating on CNFs. The fracture origins were large pores formed by insufficient sintering and scratches formed by grinding. So using CNFs coated with more SiC, the microstructures of the obtained composites became finer and the fracture origins, such large pores and scratches, became also finer.

References

1) S. Prochazka, "Special Ceramics No.6", Ed. by P. Popper, British Ceramic Research Association, Manchester, UK (1975) pp. 171–181.
2) T. T. Shin and J. Opoku, *Eng. Fract. Mech.*, 12, 479–498 (1979).
3) K. T. Faber and A. G. Evans, *J. Am. Ceram. Soc.*, 66, c-94–c-96 (1983).
4) G.-S. Xu, T. Yamakami, T. Yamaguchi, M. Endo, S. Taruta and I. Kubo, *Int. J. Appl. Ceram. Technol.*, 11, 280–288 (2014).
5) G.-S. Xu, T. Yamakami, T. Yamaguchi, M. Endo, S. Taruta and I. Kubo, *J. Ceram. Soc. Japan*, 122, 822–828 (2014).
6) Y. Morisada, M. Maeda, T. Shibayanagi and Y. Miyamoto, *J. Am. Ceram. Soc.*, 87, 804–808 (2004).
7) Y. Morisada, Y. Miyamoto, H. Moriguchi, K. Tsuduki and A. Ikegaya, *J. Am. Ceram. Soc.*, 87, 809–813 (2004).
8) Y. Morisada and Y. Miyamoto, *Mater. Sci. Eng., A*, 381, 57–61 (2004).
9) Y. Morisada, Y. Miyamoto, Y. Takaura, K. Hirota and N. Tamari, *Int. J. Refract. Met. H.*, 25, 322–327 (2007).
10) N. Ueda, T. Yamakami, T. Yamaguchi, K. Kitajima, Y. Usui, K. Aoki, M. Endo and S. Taruta, *J. Ceram. Soc. Japan*, 120, 560–568 (2012).